



This is a repository copy of *Soft rectangular sub-5 nm tiling patterns by liquid crystalline self-assembly of T-shaped bolapolyphiles*.

White Rose Research Online URL for this paper:
<http://eprints.whiterose.ac.uk/139367/>

Version: Accepted Version

Article:

Lehmann, A., Scholte, A., Prehm, M. et al. (4 more authors) (2018) Soft rectangular sub-5 nm tiling patterns by liquid crystalline self-assembly of T-shaped bolapolyphiles. *Advanced Functional Materials*, 28 (46). 1804162. ISSN 1616-301X

<https://doi.org/10.1002/adfm.201804162>

This is the peer reviewed version of the following article: A. Lehmann, A. Scholte, M. Prehm, F. Liu, X. Zeng, G. Ungar, C. Tschierske, *Adv. Funct. Mater.* 2018, 28, 1804162, which has been published in final form at <https://doi.org/10.1002/adfm.201804162>. This article may be used for non-commercial purposes in accordance with Wiley Terms and Conditions for Self-Archiving.

Reuse

Items deposited in White Rose Research Online are protected by copyright, with all rights reserved unless indicated otherwise. They may be downloaded and/or printed for private study, or other acts as permitted by national copyright laws. The publisher or other rights holders may allow further reproduction and re-use of the full text version. This is indicated by the licence information on the White Rose Research Online record for the item.

Takedown

If you consider content in White Rose Research Online to be in breach of UK law, please notify us by emailing eprints@whiterose.ac.uk including the URL of the record and the reason for the withdrawal request.



eprints@whiterose.ac.uk
<https://eprints.whiterose.ac.uk/>

Soft rectangular sub-3nm tiling patterns by liquid crystalline self-assembly of T-shaped bolapolyphiles

Anne Lehmann¹, Alexander Scholte,¹ Marko Prehm¹, Feng Liu^{*2,3}, Xiangbing Zeng³, Goran Ungar^{*3,4}, Carsten Tschierske^{*1}

¹ Department of Chemistry, Martin Luther University Halle-Wittenberg, Kurt-Mothes-Str. 2, 06120 Halle, Germany

² State Key Laboratory for Mechanical Behavior of Materials, Xi'an Jiaotong University, Xi'an 710049, P. R. China

³ Department of Materials Science and Engineering, Sheffield University, Sheffield S1 3JD, UK

⁴ Department of Physics, Zhejiang Sci-Tech University, Hangzhou 310018, China

Abstract

Square and other rectangular nano-scale tiling patterns are of contemporary interest for soft lithography. Though soft square patterns on a ~40 nm length scale can be achieved with block copolymers, even smaller tiling patterns below 5 nm can be expected for liquid crystalline phases of small molecules. However, these usually form lamellar and hexagonal morphologies and thus the challenge is to specifically design LC phases forming square and rectangular patterns, being compatible with industrial standards. Here, we report two distinct types of liquid crystalline rectangular tiling patterns occurring in a series of T-shaped p-terphenyl based bolapolyphiles. By directed side chain engineering sub-3 nm sized quadrangular honeycombs with rhombic ($c2mm$), square ($p4mm$) and rectangular ($p2mm$) shapes of the cells were formed by spontaneous self-assembly. The rectangular honeycomb with $p2mm$ lattice represents a new mode of LC self-assembly in polygonal honeycombs. In addition, pentagonal and hexagonal patterns can be obtained by molecular fine tuning.

1. Introduction

Liquid crystals (LCs) represent a prominent example of supramolecular materials that have been commercialized on a grand scale, especially in display technology.^{1,2} However, they also provide access to nano-scale patterning on the sub-10 nm length scale^{3,4} for use in selective membranes,^{5,6,7} in soft nanolithography,⁸ for ion conduction,⁹ as well as for organic electronic applications.^{10,11,12,13,14} Moreover, LCs provide significant fundamental insights into phase transition phenomena and the development of order, chirality^{15,16} and complexity in soft condensed matter.¹⁷ In recent years the complexity of the self-assembled LC superstructures has been significantly increased, for example, by reduced molecular symmetry based on chirality,^{18,19} by introduction of steric and geometrical frustration,^{20,21} by the transition from amphiphilicity to polyphilicity^{22,23,24} and by the incorporation of nano-particles into LC templates.^{25,26,27}

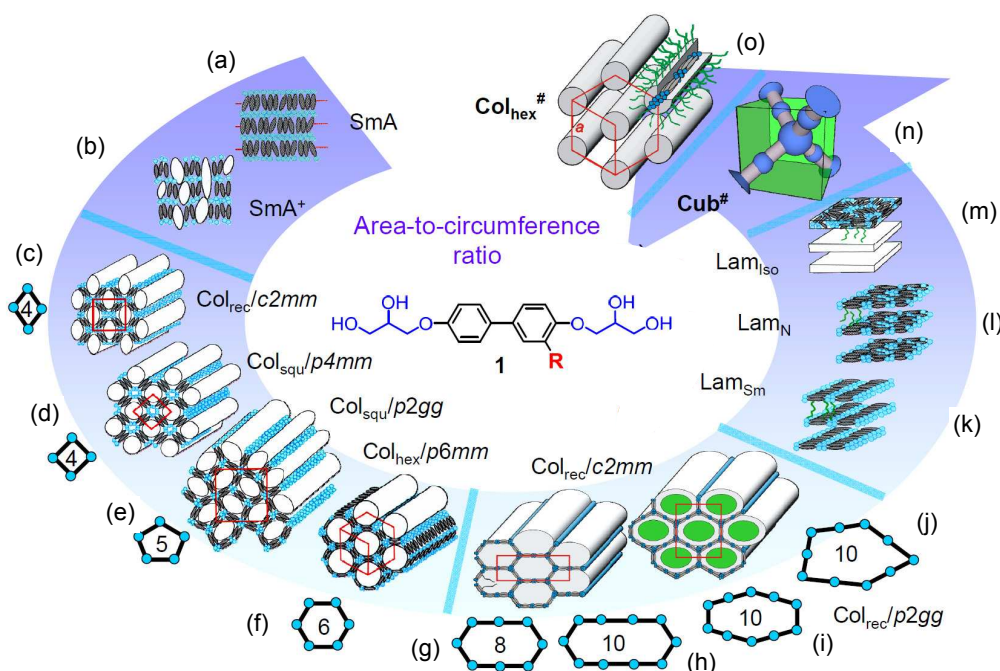


Figure 1. Liquid crystalline self-assembly of laterally substituted biphenyl based bolapolyphiles **1** depending on the lateral chain ($R = (O)C_nH_{2n+1}$) volume. The segregation of the lateral chains leads to domain formation which distorts the simple lamellar organization ($a \rightarrow b$) and then leads to polygonal honeycombs (c-f), giant honeycombs formed by end-to-end connected pairs of molecules (g-j), lamellar phases with coplanar rod alignment (k-m) as well as cubic network phases (n) and columnar phases formed by coaxial rod-bundles (o); structures (n,o) require branched chains.^{17,30}

T-shaped polyphiles composed of a rigid and linear aromatic core, functionalized at each end with a glycerol group and laterally with one or two non-polar and flexible chains represent an especially successful class of mesogenic materials forming a broad variety of different new

1 LC superstructures.^{28,29,30} For example, the biphenyl based compounds **1/n** have been shown
2 to form a series of LC honeycombs with different cross-section shapes of the prismatic cells
3 ranging from rhombic via pentagonal to hexagonal (Fig. 1c-f).²⁸ In these honeycombs the
4 hydrogen bonding networks of the glycerols are organized in columns which are connected by
5 ribbons of aromatic cores forming the walls of a honeycomb; the resulting cells are filled by
6 the lipophilic lateral chains. For molecules with bulkier branched, semiperfluorinated or
7 carbosilane chains attached to the biphenyl core giant honeycombs were observed, with some
8 double-length walls composed of pairs of end-to-end connected molecules (Fig. 1g-j).^{31,32}
9 Further increasing the side-chain volume leads to lamellar phases with the rod-like cores lying
10 parallel to the layer planes (Fig. 1k-m),^{33,34,35,36} followed by different types of axial rod-
11 bundle phases with hexagonal or cubic symmetry (Fig. 1n, o).^{37,38,39,40} Recent simulation work
12 supported the proposed self-assembly of these polyphilic LC compounds.^{41,42,43,44,45,46}

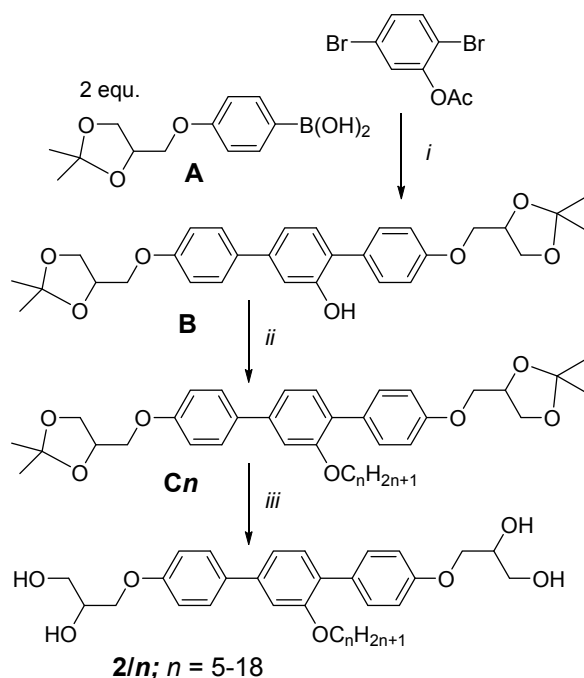
13
14
15
16
17
18
19
20
21
22 Among the tiling patterns, rectangular nanoscale patterns on a length scale well below
23 that achievable with block copolymers (~40 nm) are of present interest in microelectronic
24 industry for soft lithography, because these structures, in contrast to the more common
25 hexagonal patterns, are compatible with the industrial standards, as they can produce the x-y
26 matrices for devices.^{8,47,48} Though smaller high- χ -low- N -block co-oligomers³ and also
27 classical liquid crystalline materials involving rod-like or disc-like units⁴ lead to patterns on a
28 sub-10 nm length scale,^{49,50} so far predominantly lamellar and hexagonal patterns were
29 obtained in this way. Even compounds with a square molecular shape usually form hexagonal
30 lattices, because the soft periphery of alkyl chain allows space and time averaged rotational
31 disorder around the column long axes. A remarkable exception is provided by porphyrins
32 which were shown to organize into square and rectangular columnar LC and soft crystalline
33 phases in some cases;^{51,52} here, the aromatic cores are arranged on the square lattice,
34 embedded in a continuum formed by the flexible alkyl chains. Soft square patterns with
35 inverted structure, i.e. the fluid chains forming the cores and rigid π -conjugated rods forming
36 a square honeycomb around them, were reported for liquid crystalline assemblies of the above
37 mentioned T- and X-shaped polyphiles.^{24,53,54,55} In this case rotational averaging is inhibited by
38 the restrictions provided by the network structure of the honeycomb. However, in polyphiles
39 of this type, with relatively short rod units, hexagonal and pentagonal honeycombs are
40 dominant (Fig. 1e,f),^{28,29,30,31} whereas square cells (Fig. 1d) were only found under special
41 circumstances in small temperature ranges.^{28,56}

42
43
44
45
46
47
48
49
50
51
52
53
54
55
56
57
58 Herein we present a new series of T-shaped polyphilic compounds **2/n**, based on the *p*-
59 terphenyl core^{53,57,58,59} and having a single normal alkyl lateral chain C_nH_{2n+1} grafted to the
60
61
62
63
64
65

middle benzene ring (see Table 1). In the **2/n** series the chain length was varied from $n = 5$ to 22. For several compounds of this series with intermediate chain length ($n = 8-11$) three distinct liquid crystalline (LC) quadrangular tiling patterns were found. Beside the previously known square and rhombic honeycombs a new rectangular honeycomb with reduced plane group symmetry $p2mm$ was discovered. That the distinct structures were observed in a single series of compounds depending on lateral alkyl chain length and temperature demonstrates the power of lateral chain engineering for precise morphological control of rectangular sub 3nm patterns by molecular self-assembly in LC soft matter.^{17,29,60,61}

2. Results and Discussion

2.1 Synthesis



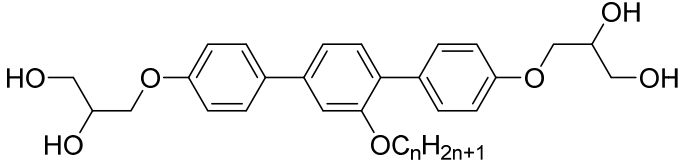
Scheme 1. Synthesis of compounds **2/n**; Reagents and conditions: (i) 1. Pd(PPh₃)₄, THF, H₂O, NaHCO₃, reflux, 12 h; 2. NaOH, H₂O, 25 °C, 12 h; (ii) K₂CO₃, DMF, 80 °C, 12 h; (iii) PPTS, MeOH, THF, 50 °C, 24 h; for details, see SI.

Compounds **2/n** were synthesized as shown in Scheme 1. The key intermediate is the p-terphenyl-2'-ol **B** which was obtained in a Suzuki cross coupling⁶² between the substituted benzene boronic acid **A**^{63,64} and 2,5-dibromophenylacetate^{65,66} followed by hydrolytic deprotection of the phenolic OH group.⁵⁷ Etherification of **B** with n -alkyl bromides yielded the acetonides **C_n** which were then deprotected. The synthetic procedures and analytical data of all compounds **2/n** are collated in the SI.

2.2 Investigation of self-assembly

The obtained compounds were investigated by polarizing microscopy (POM), differential scanning calorimetry (DSC) and X-ray scattering (SAXS and WAXS); the details of the methods used are given in the SI and the observed LC phases and phase transitions are collated in Tables 1, S1 and S6.

Table 1. Data on compounds **2/n**.^a



2/n	$T/^\circ\text{C}$, [$\Delta H/\text{kJ}/\text{mol}^{-1}$]	d or a , b/nm ($T/^\circ\text{C}$)	n_{cell}	n_{wall}
2/5	Cr 125 [10.2] SmA+ 159 [1.7] Iso	$d_1 = 2.14$ (150) $d_2 = 2.47$	-	-
2/7	Cr 130 [20.4] SmA+ 137 [1.2] Iso	$d_1 = 2.10$ $d_2 = 2.48$ (120)	-	-
2/8	Cr 137 [16.0] Col _{rec} / $c2mm$ 140 [2.9] Iso	3.91, 3.83 (135)	8.4	2.1
2/9	Cr 109 [18.5] Col _{squ} / $p4mm$ /Col _{rec} / $p2mm$ ^b 138 [-] Col _{squ} / $p4mm$ 154 [4.0] Iso	2.74 (125) 2.41 3.13 (127)	4.1 4.1	2.0 2.1
2/10	Cr 114 [13.4] Col _{rec} / $p2mm$ 123 [0.2] Col _{squ} / $p4mm$ 160 [4.7] Iso	2.68 (145) 2.39, 3.13 (110)	3.8 3.9	1.9 2.0
2/11	Cr 102 [9.1] Col _{rec} / $p2mm$ 122 [0.2] Col _{squ} / $p4mm$ 162 [4.5] Iso	2.70 (135) 2.38, 3.10 (115)	3.6 3.7	1.8 1.9
2/12	Cr 102 [9.2] Col _{rec} / $p2gg$ 154 [4.3] Iso	6.88, 6.44 (150)	22.4	2.2
2/14	Cr 77 [9.6] Col _{rec} / $p2gg$ 160 [5.4] Iso	6.89, 6.46 (115)	20.9	2.1
2/15	Cr 81 [10.4] Col _{rec} / $p2gg$ 165 [6.1] Iso	6.86, 6.49 (155)	20.8	2.1
2/16	Cr 64 [9.2] Col _{hex} / $p6mm$ 164 [5.8] Iso	4.26 (160) 4.34 (100)	7.4 7.0	2.5 2.3
2/18	Cr 102 [8.6] Col _{hex} / $p6mm$ 177 [7.2] Iso	4.25 (160) 4.30 (120)	6.9 6.6	2.3 2.2
2/22	Cr 34 [26.2] Col _{hex} / $p6mm$ 183 [6.7] Iso	4.24 (160) 4.32 (80)	6.1 6.0	2.0 2.0

^aTransition temperatures were taken from the first DSC heating scan (10 K min⁻¹, peak temperatures, see Figure S2); only the highest melting point and the total of all melting and Cr-Cr transitions are shown; for these transitions and the phase transitions on cooling, see Table S1; Abbreviation: SmA+ = strongly distorted lamellar phase; Col_{rec}/ $c2mm$ = rhombic LC honeycomb with $c2mm$ symmetry; Col_{squ}/ $p4mm$ = square LC honeycomb; Col_{rec}/ $p2mm$ = rectangular LC honeycomb; Col_{rec}/ $p2gg$ = pentagonal LC honeycomb with $p2gg$ symmetry; Col_{rec}/ $p6mm$ = hexagonal LC honeycomb; n_{cell} , number of molecules in a unit cell with h corresponding to the d -value of the wide angle scattering, n_{wall} = average thickness of the honeycomb walls (for details of the calculation, see Table S6). ^bCol_{squ}/ $p4mm$ /Col_{rec}/ $p2mm$ = square honeycomb showing surface induced deformation to rectangular honeycombs.

2.3 SmA+ phases

As typical for T-shaped polyphiles, compounds **2/n** with relatively short lateral chains ($n \leq 7$) form a lamellar phase, characterized by a highly birefringent fan-like texture between crossed polarizers (Fig. 2a). Shearing gives rise to an isotropic appearance in the shear induced homeotropic areas (layers parallel to the substrate surface) with additional oily streaks, due to defects, thus indicating a uniaxial smectic phase (see inset in Fig. 2a).

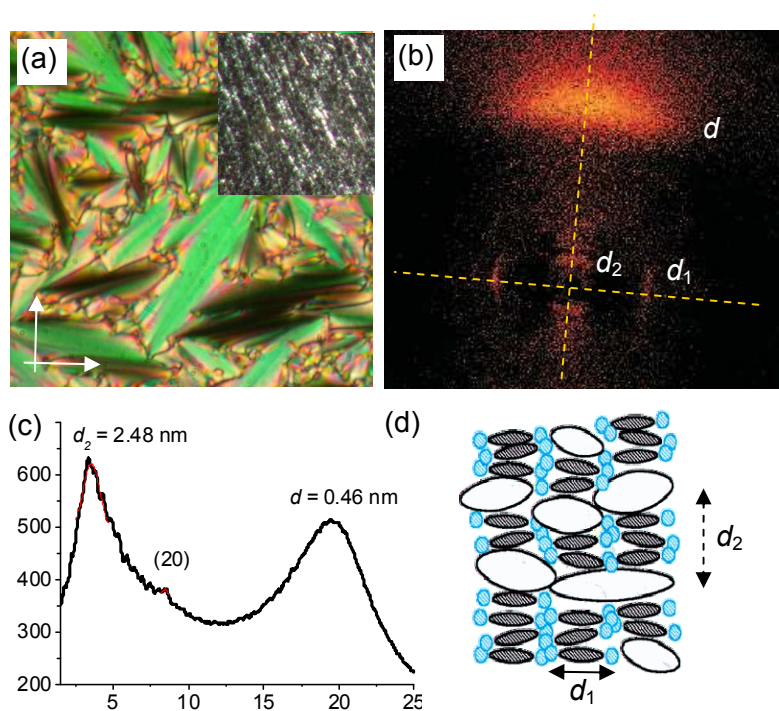


Figure 2. The SmA+ phase of compound **2/7**. (a) Texture at $T = 120$ °C as observed between crossed polarizers, showing the fan-texture in planar alignment; the inset shows the texture after shearing, being homeotropically aligned, thus appearing dark with birefringent defects (oily streaks); (b) XRD pattern of a surface aligned sample at the same temperature after subtraction of the scattering pattern in the isotropic liquid state; (c) scan over the original scattering pattern (see Fig. S10) and (d) model of the phase structure, blue = glycerols, gray = terphenyls and the white ellipses indicate the disordered domains of the lateral alkyl chains; for XRD data of compound **2/5**, see Fig. S9.

In the XRD patterns of surface aligned samples (X-ray beam parallel to the horizontal surface) the wide angle diffraction is diffuse with a maximum at $d = 0.46$ nm (using Bragg equation) and located on the meridian (Fig. 2b). This indicates a LC phase with the *p*-terphenyl long axes predominantly parallel to the surface (planar alignment). In the small angle region there are sharp diffraction arcs on the equator, i.e. perpendicular to the direction of the diffuse wide angle scattering, with a distance $d_1 = 2.1$ - 2.2 nm (Fig. 2b). d_1 is close to the molecular length as measured between the two secondary OH groups of the glycerol units ($L_{\text{mol,min}} = 2.3$ nm; see Fig. S21a). Hence, d_1 can be assigned to the layer spacing of a

1
2
3
4
5
6
7
8
9
10
11
12
13
14
15
16
17
18
19
20
21
22
23
24
25
26
27
28
29
30
31
32
33
34
35
36
37
38
39
40
41
42
43
44
45
46
47
48
49
50
51
52
53
54
55
56
57
58
59
60
61
62
63
64
65

monolayer lamellar structure where the terphenyls are organized on average perpendicular to the layer planes (SmA). The slightly reduced d -value compared to the length of the fully extended molecule is mainly attributed to the reduced orientational order parameter (some random tilt of the terphenyls) due to the distortion of parallel alignment by the lateral chains (Fig. 2d). In addition the partial intercalation of the glycerols can reduce layer frustration caused by the lateral separation of the terphenyls by the intercalated alkyl side-chains. The scattering intensity of the layer reflection is comparatively weak, due to the low electron density difference between glycerols and terphenyls (see Figs. 3d and 4d,g).^{28,64} There is an additional diffuse small angle scattering blob with a maximum at $d_2 = 2.5$ nm on the meridian, i.e. in the direction of the wide angle scattering maximum (Fig. 2b,c). This scattering indicates an additional short range in-plane periodicity which is assumed to arise from local aggregation of the alkyl chains tethered to the aromatic cores, as previously proposed for lamellar phases with strongly distorted layers and termed SmA+ phase (Fig. 2d).^{28,64} The alkyl chain domains are still randomly distributed (random mesh phases⁶⁷), hence the small angle scattering is diffuse.

2.4 Col_{rec}/c2mm phase - rhombic honeycomb

Compound **2/8** forms a highly birefringent spherulitic-like texture (Fig. 3a) as typical for columnar phases, suggesting that the nano-segregated alkyl chain domains now adopt a long range 2D periodic order. In the SAXS pattern of an aligned sample (Fig. 3a) the wide angle scattering is still diffuse and has its maximum at $d = 0.46$ nm. In the following this value is used as the height (h) of the unit cell. The SAXS pattern can be indexed to a centred rectangular 2D lattice (c2mm) with the lattice parameters $a = 3.9$ and $b = 3.8$ nm (see Fig. 3e). There is thus only a slight distortion from a square lattice. The lattice parameters are close to $\sqrt{2} \times L_{\text{mol,max}}$ where $L_{\text{mol,max}} = 2.6\text{-}2.7$ nm is the molecular length in the most stretched conformation between the ends of the primary OH groups (see Fig. S21b). This is in line with a honeycomb formed by rhombic cells where a and b are the long and the short diagonal of the rhombus. Such structure is corroborated by the electron density (ED) map shown in Fig. 3d. The high ED areas containing the p -terphenyls and glycerols (blue, purple) form a honeycomb with the resulting rhombic prismatic cells filled by the low ED alkyl chains (red/yellow/green). As the calculated number of molecules per “unit cell” with $h = 0.46$ nm thickness is $n_{\text{cell}} = 8.4$ (Table 1, for calculation see Table S6), there are about 4 molecules forming the walls around each prismatic cell, and therefore, two back-to-back arranged p -

1
2
3
4
5
6
7
8
9
10
11
12
13
14
15
16
17
18
19
20
21
22
23
24
25
26
27
28
29
30
31
32
33
34
35
36
37
38
39
40
41
42
43
44
45
46
47
48
49
50
51
52
53
54
55
56
57
58
59
60
61
62
63
64
65

terphenyls form one “brick” or one stratum of each of the four walls ($n_{\text{wall}} = 2.1$; “double walls”, see Fig. 3e,f and Tables 1 and S6). This $c2mm$ phase can be considered as derived from the SmA+ phase by establishment of long-range order caused by the expansion of the alkyl domains and their coalescence into nano-segregated columns⁶⁴ (Fig. 3e, f).

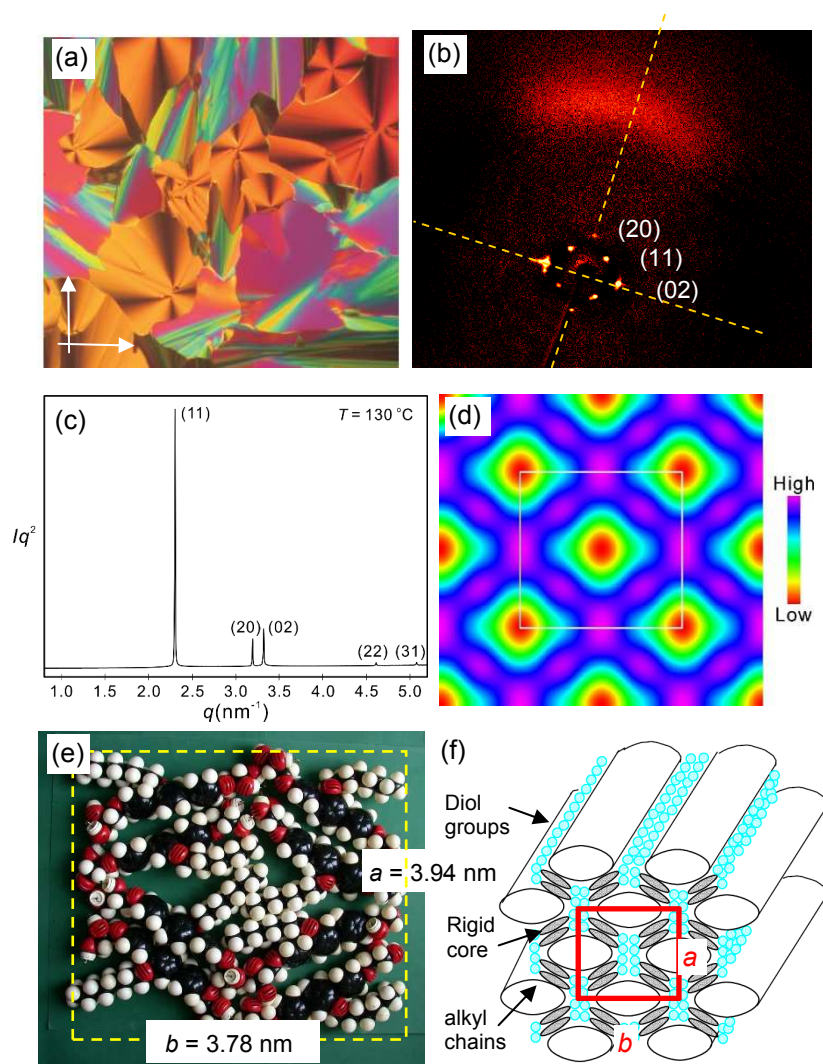


Figure 3. The rhombic LC honeycomb ($\text{Col}_{\text{rec}}/c2mm$) of compound **2/8**: a) Texture (crossed polarizers, direction of polarizer/analyzer shown with arrows) at $T = 136$ °C; b) XRD pattern of a surface aligned sample at $T = 135$ °C after subtraction of the scattering pattern in the isotropic liquid state (for original diffraction pattern, see Fig. S11); c) SAXS powder pattern (synchrotron source); d) ED map reconstructed from c) (for details, see SI); e) molecular models and f) schematic model showing the organization of the molecules.

2.5 $\text{Col}_{\text{sq}}/p4mm$ phase – square honeycombs

On cooling from the isotropic liquids, compounds **2/9** – **2/11** also show spherulitic textures in areas of planar alignment (columns in sample plane) (Figs. 4c, 5a and S4a). The dark areas, in which the columns are aligned perpendicular to the surfaces, indicate that the columnar

1 phase is uniaxial, i.e. of either hexagonal or square symmetry. On slow cooling the formation
2 of rectangular 4-star figures can be observed, which is a first indication of square symmetry of
3 the developing lattice (see inset in Fig. 4c). In this mesophase the birefringence is negative as
4 confirmed by polarizing microscopy with a λ -retarder plate (see insets in Fig. 5a), meaning
5 that the main π -conjugation pathway, i.e. the direction of the terphenyl cores, is perpendicular
6 to the column long axis, as is typical for polygonal honeycomb LCs. The SAXS pattern of this
7 phase can be indexed to a square $p4mm$ lattice with $a_{\text{squ}} = 2.7$ nm (see Fig. 4a,b). Notably, the
8 lattice parameter does not change significantly upon increasing the side-chain length. That the
9 parameter a_{squ} is close to the maximum molecular length $L_{\text{mol,max}} = 2.6$ - 2.7 nm in all cases, is
10 in line with the proposed square honeycomb structure. This structure was corroborated by ED
11 reconstruction of high resolution XRD patterns (synchrotron source, see Fig. S8b). As shown
12 in Fig. 4d there are square shaped low electron density areas (red to green) assigned to the
13 prismatic cell interior containing the alkyl chains. These are framed by a net of high electron
14 density squares (blue/purple) formed by terphenyl partition walls connected at the vertices by
15 the glycerol groups. As in the $c2mm$ phase, the walls contain on average two terphenyls back-
16 to-back ($n_{\text{wall}} \sim 2$, see Table 1) which allows all side-chains easy access to the prismatic cell
17 interior. The viability of the packing model and the efficiency of space filling is confirmed by
18 molecular dynamics simulation (see Fig. S1 and associated explanations). Overall, the
19 structures of the $c2mm$ and $p4mm$ phases are very similar, the difference being that the angles
20 lock in at 90° in the square phase. The larger volume of the lateral chains of compounds **2/9-**
21 **2/11** evidently require the larger volume that a square honeycomb provides.
22
23
24
25
26
27
28
29
30
31
32
33
34
35
36
37
38
39
40
41
42
43
44
45
46
47
48
49
50
51
52
53
54
55
56
57
58
59
60
61
62
63
64
65

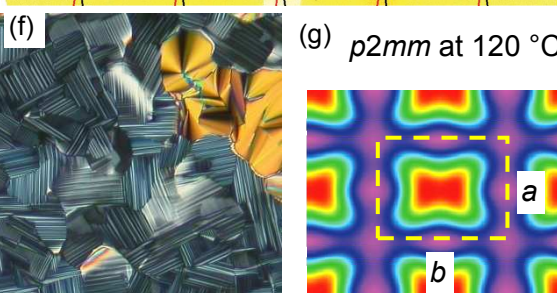
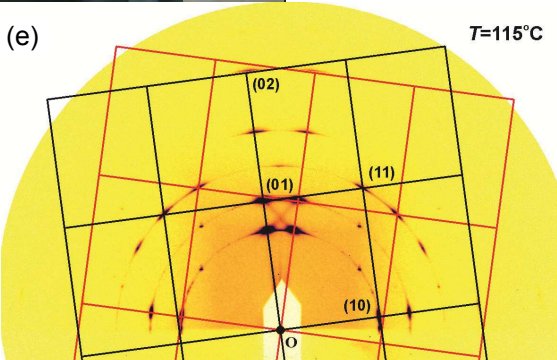
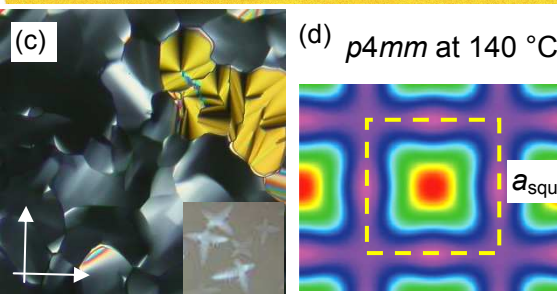
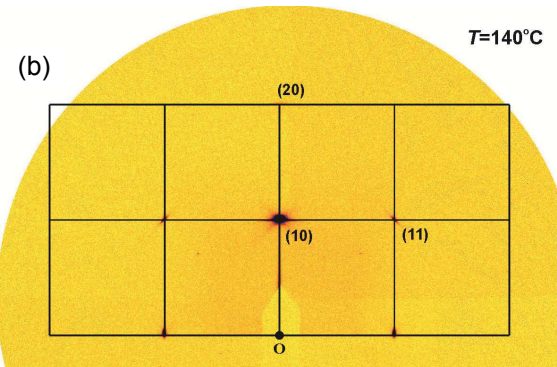
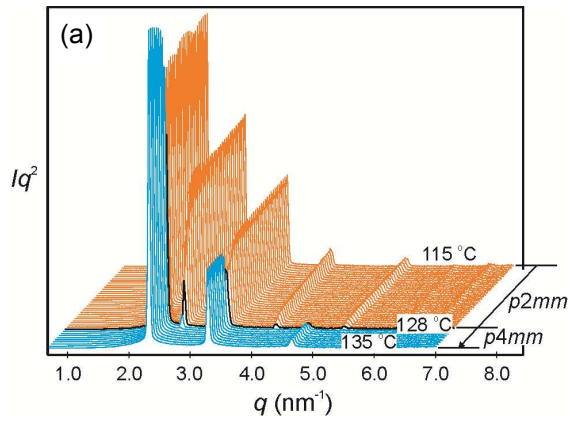


Figure 4. Square and rectangular cylinder phases of compound **2/11**: a) temperature evolution of the powder SAXS curve (synchrotron source), b) GISAXS pattern of the $Col_{squ}/p4mm$ phase of an aligned sample at $T = 140$ °C; c) texture (crossed polarizers) at the same

1 temperature; the inset shows the growth of 4-star figures upon slow cooling from Iso at $T =$
2 162 °C; d) ED map reconstructed from the powder pattern (Fig. S8b); e) GISAXS pattern of
3 an aligned sample of the $\text{Col}_{\text{rec}}/p2mm$ phase at $T = 115$ °C; (only one orientation is shown, red
4 and black lattice represent two mirrored domains respectively); f) texture (crossed polarizers)
5 at the same temperature and g) ED map reconstructed from the powder pattern (Fig. S8a); for
6 data of **2/10**, see Figs. S3a-d and S13.
7

9 **2.6 $\text{Col}_{\text{rec}}/p2mm$ phases of compounds **2/10** and **2/11** – rectangular honeycombs**

12 Compounds **2/10** and **2/11** show an additional phase transitions with a small enthalpy
13 (0.2 kJ mol^{-1}) from this square honeycomb to a low temperature LC phase (Table 1). At this
14 transition the birefringence of the spherulitic texture increases and the dark homeotropic areas
15 become birefringent with development of a typical 90° crossed stripe pattern (Fig. 4c,f). There
16 is no change in the WAXS, which remains diffuse (see Fig. S13), whereas the SAXS pattern
17 changes abruptly at this phase transition (Fig. 4a). The diffraction pattern of the low
18 temperature phase of **2/11**, for example, can be indexed to a non-centred rectangular lattice
19 ($\text{Col}_{\text{rec}}/p2mm$) with parameters $a = 2.38 \text{ nm}$ and $b = 3.10 \text{ nm}$ (Fig. 4e). a is close to the
20 molecular length measured between the secondary OH groups in a compact conformation of
21 the glycerols ($L_{\text{mol,min}} = 2.3 \text{ nm}$, see Fig. S21a), whereas b exceeds considerably the maximum
22 molecular length ($L_{\text{mol,max}} = 2.6\text{-}2.7 \text{ nm}$, see Fig. S21b). However, the area of the $p2mm$ unit
23 cell (7.4 nm^2) remains almost the same or is even slightly increased compared to that of the
24 corresponding $p4mm$ phase (7.3 nm^2), see Table S6. At the $p4mm \rightarrow p2mm$ transition (Fig.
25 4d,g) the prismatic cells expand along b and shrinks along a (Table S6). As the cell volume
26 does not substantially change at the $p4mm - p2mm$ transition thermal expansion/shrinkage
27 could not be the major reason for this phase transition. It is more likely that the transition
28 from square to rectangular prismatic cells is caused by an increased *trans* fraction of the alkyl
29 chains at reduced temperature, though the chains remain in a liquid-like fluid state as
30 confirmed by the diffuse WAXS (Fig. S13). This supports an anisotropic orientation of the
31 chains with increased preference for them to lie parallel and thus supporting a deformation of
32 the cells. As the parameter $b = 3.1 \text{ nm}$ exceed the maximum molecular length of $2.6\text{-}2.7 \text{ nm}$,
33 the glycerols units of molecules along a have to be intercalated between the polar groups of
34 the molecules aligned along b , leading to a strongly elliptical shape of the polar columns
35 involving the hydrogen bonding glycerols (Fig. S22). This reduces the parameter a and
36 simultaneously increases the number of molecules organized laterally side-by-side in the
37 honeycomb wall along the shorter direction a . This enhancement of the walls along a takes
38 place on expense of the molecules forming the walls in direction b , thus leading to a slightly
39
40
41
42
43
44
45
46
47
48
49
50
51
52
53
54
55
56
57
58
59
60
61
62
63
64
65

1 different number of molecules in the lateral cross section of the walls along a and b (Fig. 4g),
2 while, the overall average number of molecules per unit cell remains almost the same as in the
3 $p4mm$ lattice
4
5

6 **2.7 The surface induced Col_{rec}/ $p2mm$ phase of compound 2/9**

7
8
9

10 Compound **2/9**, being at the boundary between rhombic and square/rectangular prismatic
11 cells, behaves differently. Similar to compounds **2/10** and **2/11** a $p4mm$ phase (indicated by
12 POM and XRD, see Fig. 5) is found at high temperature and a transition from a uniaxial to a
13 birefringent (biaxial) texture is observed by polarizing microscopy on cooling (Fig. 5a,c).
14 However, in contrast to compounds **2/10** and **2/11** this optical texture change is neither
15 associated with a transition enthalpy (see DSC in Fig. S2d-f) nor with a stepwise change in
16 position of the SAXS peaks in the powder pattern recorded on the bulk material on cooling
17 (Figs. 5e and S7b); nor is there any change in WAXS, which remains completely diffuse (Fig.
18 S12). However, in GISAXS experiments (Fig. 5b,d), where a thin films with predominately
19 homeotropic alignment was investigated on silicon surface, additional reflections of a $p2mm$
20 rectangular lattice appear at the transition temperature of 138 °C beside the still strong
21 reflections of the square lattice ($a_{\text{squ}} = 2.74$ nm). At 127 °C the rectangular lattice parameters
22 are $a = 3.13$ nm and $b = 2.41$ nm. These parameters are almost the same as measured for **2/10**
23 and **2/11** (see Table 1). However, it appears that for **2/9** the $p4mm \rightarrow p2mm$ transition requires
24 the support by surface anchoring, whereas the bulk structure remains $p4mm$. Obviously, the
25 shorter chains of **2/9** provide a weaker driving force for deformation of the square honeycomb
26 and we propose that the higher $p4mm$ symmetry could be maintained by some out-of-plane
27 distortion of the otherwise flat honeycomb lattice. Various modes of “escape in the third
28 dimension” have been found in the soft LCs on different length scales to resolve the effects of
29 frustration. It would appear that at the surfaces the honeycomb could be pinned to the polar
30 substrate sufficiently by its glycerol groups that the out-of-plane distortion is suppressed
31 strongly and the square lattice is deformed to escape steric frustration. The improved parallel
32 alignment of the alkyl chains achieved in the rectangular lattice supports the $p4mm$ - $p2mm$
33 transition.
34
35
36
37
38
39
40
41
42
43
44
45
46
47
48
49
50
51
52
53
54
55
56
57
58
59
60
61
62
63
64
65

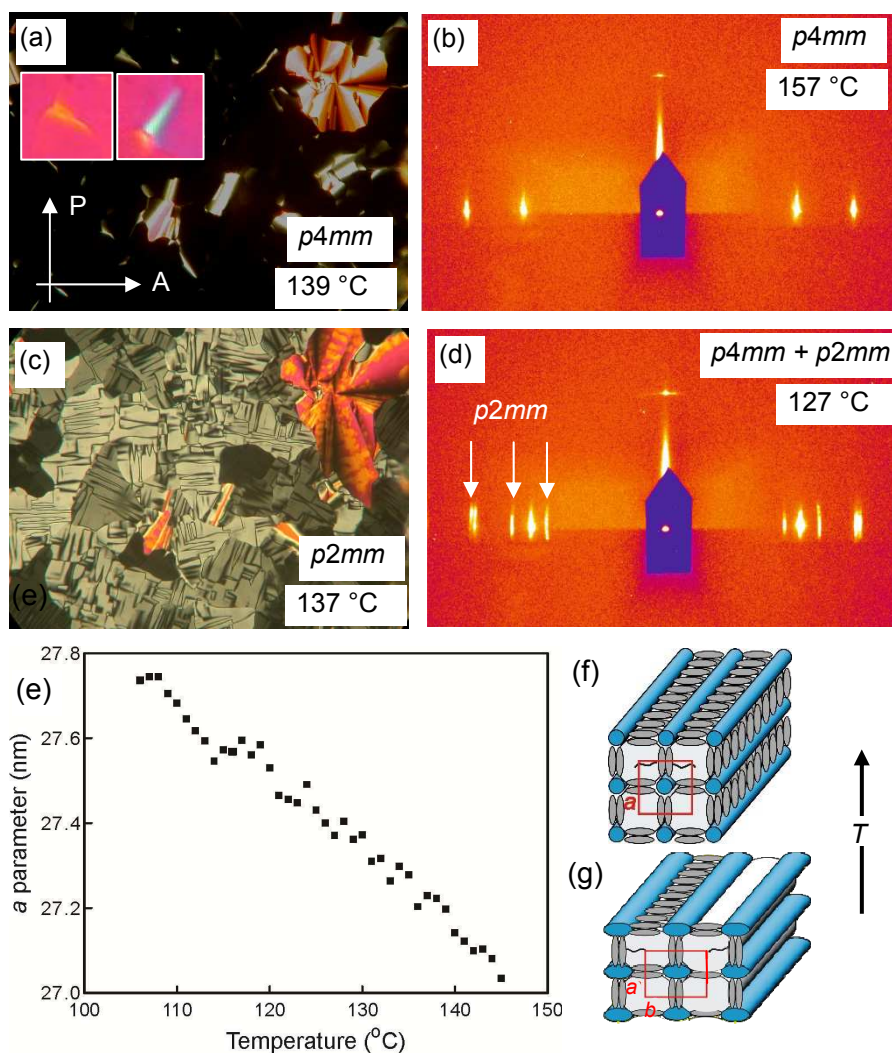


Figure 5. The rectangular LC honeycombs of compound **2/9**. a,c) Textural changes as observed for the $Col_{squ}/p4mm$ phase upon cooling between crossed polarizers, showing the emergence of birefringence in the optically isotropic areas (columns perpendicular to the surfaces) due to the transition to $Col_{rec}/p2mm$; the insets in a) show birefringent domains with λ -retarder plate and the slow axis in the direction SW-NE, indicating negative birefringence. b,d) GISAXS patterns at different temperatures, showing in b) the $p4mm$ phase and in d) the coexistence of $p4mm$ and $p2mm$ in the surface films; e) temperature dependence of the lattice parameter in the $p4mm$ phase between 145 and 105 °C; f,g) schematic models of the $p4mm$ and $p2mm$ phases; for additional data, see Figs. S6 and S7.

2.8 Pentagonal and hexagonal honeycombs of compounds 2/12 – 2/22

For compounds **2/12** - **2/15** with still larger lateral chains the square honeycombs cannot accommodate the chain volume and instead formation of another rectangular columnar phase is observed, this time with $p2gg$ symmetry. This lattice representing a honeycomb composed of slightly deformed pentagonal prismatic cells (Fig. 6a,c,e).⁶⁸ While a honeycomb composed of distorted pentagons can also form a square lattice with $p4gm$ symmetry, when the chains

are not quite large enough to fill the required space the symmetry is reduced from $p4gm$ to $p2gg$ ^{28,56} and a and b parameters converge as chain length increases (Table 1).

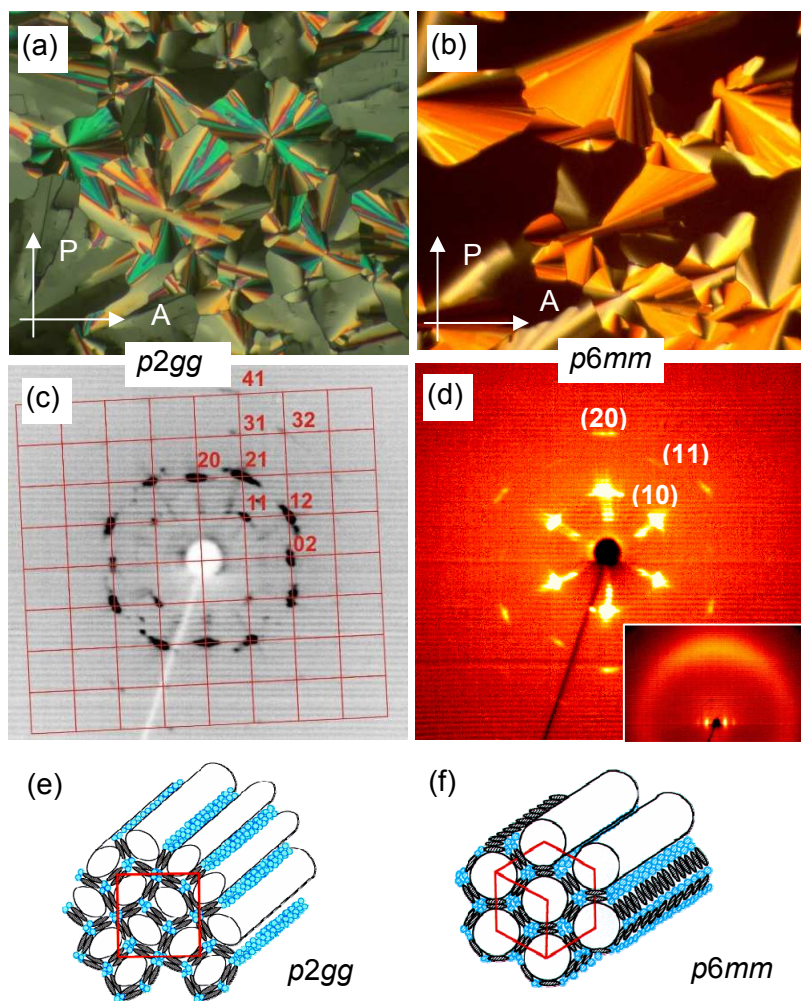


Figure 6. The pentagonal and hexagonal honeycombs. a,b) Textures; c,d) 2D-SAXS patterns of aligned samples with indexation, and e,f) schematic models of the LC honeycombs. a) $Col_{rec}/p2gg$ phase of compound **2/14** at $T = 157$ °C; c) $Col_{rec}/p2gg$ phase of **2/12** at $T = 150$ °C; b) $Col_{hex}/p6mm$ phase of **2/16** at $T = 165$ °C; d) $Col_{hex}/p6mm$ phase of **2/16** at $T = 160$ °C; in c and d) alignment is planar; the inset in d) shows the WAXS pattern of a sample with homeotropic alignment as obtained upon very slow cooling; in all cases the X-ray beam is parallel to the substrate. The texture in b) shows black areas with homeotropic alignment, other highly birefringent spherulitic domains in a) and b) have planar alignment); for additional data, see Figs. S5, S14-S20 and Table S6.

Compounds **2/16** - **2/22** with the longest chains form the hexagonal columnar phase (Fig. 6b,d,f). The hexagonal lattice parameter is around $a_{hex} = 4.3$ nm for all of these compounds, corresponding to $a_{hex} = \sqrt{3}L_{mol}$ as is typical for hexagonal honeycomb LCs. For the hexagonal phase of **2/16** the alignment of the honeycombs can be either planar (Fig. 6d) or, upon very slow cooling (<0.1 K min^{-1}), homeotropic, as confirmed by the 2D SAXS patterns (see inset in Fig. 6d and Figs. S17, S18). This demonstrates that uniform alignment of

1
2
3
4
5
6
7
8
9
10
11
12
13
14
15
16
17
18
19
20
21
22
23
24
25
26
27
28
29
30
31
32
33
34
35
36
37
38
39
40
41
42
43
44
45
46
47
48
49
50
51
52
53
54
55
56
57
58
59
60
61
62
63
64
65

macroscopic domains of the polygonal honeycomb LCs, either planar or homeotropic, can be achieved by changing preparation conditions.

3. Summary and Conclusions

The T-shaped *p*-terphenyl based bolapolyphiles **2/n** show a sequence of six different LC phases depending on chain length and temperature. With increasing lateral chain length the random mesh lamellar phase (SmA+) is replaced by a series of successive LC honeycombs with rhombic (*c2mm*), square/rectangular (*p4mm/p2mm*), pentagonal (*p2gg*) and hexagonal (*p6mm*) cells. However, no triangular honeycomb is found between SmA+ and the quadrangular honeycombs. The reason might be that the tight 60° vertices in the triangular cells, if formed by the relatively short *p*-terphenyls, are difficult to access by the lateral alkyl chains; such corners would likely present entropic depletion regions. Only for longer rod-like units this effect becomes sufficiently insignificant to allow the formation of stable triangular honeycombs.^{24,69,70} This unfavourable acute angle effect might also explain why the rhombic honeycomb (*c2mm*) is found in only one homologue and has an almost square shape. Compared to the biphenyl based bolapolyphiles **1/n** involving shorter aromatic cores (Fig. 1b-f),^{28,29,30} here for terphenyls, to keep the equivalent area-to-circumference ratio, the different honeycomb types are shifted towards longer alkyl chains (e.g. pentagons: from $10 \leq n \leq 12$ to $12 \leq n \leq 15$; hexagons: from $n \geq 12$ to $n \geq 16$). The deformation of the square honeycombs to a rectangular one (*p2mm*) is also attributed to increasing anisotropy due to growing contribution of straight and parallel *all-trans* segments at lowered temperature. These rectangular honeycombs represent a new type of LC honeycombs, expanding the range of existing liquid crystalline quadrangular tilings.^{28,64,71} For the two compounds with longer chains ($n = 10,11$) the temperature dependent square symmetry breaking is spontaneous, whereas for shorter chains ($n = 9$) it requires additional surface anchoring.

Overall, liquid crystalline square and rectangular tiling patterns on a sub-3 nm scale with potential for application in soft nano-lithography were obtained by molecular design. This work provides a proof of concept by using model T-shaped molecules based on a simple *p*-terphenyl unit which can be extended to other π -conjugated systems. These quadrangular soft arrays of π -conjugated aromatics could also be of potential interest for the morphological design and patterning of self-assembled organic electronic materials.

Acknowledgements

This work was supported by the DFG (392435074), the National Natural Science Foundation of China (No. 21761132033 and 21374086) and EPSRC (EP-P002250). The authors thank beamlines BL14B1 and BL16B1 (Shanghai Synchrotron Radiation Facility), BM28 at ESRF and I22 at Diamond Light Source for providing the beam time.

References

- 1 J. F. Stoddart, Thither supramolecular chemistry, *Nature Chemistry* **2009**, *1*, 5-15.
- 2 N. Koide, *The Liquid Crystal Display Story*, Springer Tokyo **2014**.
- 3 C. Sinturel, F. S. Bates, M. A. Hillmyer, High χ -Low-*N* Block Polymers: How Far Can We Go? *ACS Macro Lett.* **2015**, *4*, 1044–1050.
- 4 K. Nickmans, A. P. H. J. Schenning, Directed Self-Assembly of Liquid-Crystalline Molecular Building Blocks for Sub-5 nm Nanopatterning, *Adv. Mater.* **2018**, *30*, 1703713.
- 5 X. Feng, M. E. Tousley, M. G. Cowan, B. R. Wiesenauer, S. Nejadi, Y. Choo, R. D. Noble, M. Elimelech, D. L. Gin, C. O. Osuji, Scalable Fabrication of Polymer Membranes with Vertically Aligned 1 nm Pores by Magnetic Field Directed Self-Assembly, *ACS Nano* **2014**, *8*, 11977–11986.
- 6 S. Bhattacharjee, J. A. M. Lugger, R. P. Sijbesma, Tailoring Pore Size and Chemical Interior of near 1 nm Sized Pores in a Nanoporous Polymer Based on a Discotic Liquid Crystal, *Macromolecules* **2017**, *50*, 2777–2783.
- 7 C. Li, J. Cho, K. Yamada, D. Hashizume, F. Araoka, H. Takezoe, T. Aida, Y. Ishida, Macroscopic ordering of helical pores for arraying guest molecules noncentrosymmetrically *Nat. Commun.* **2015**, *6*, 8418.
- 8 C. Tang, E. M. Lennon, G. H. Fredrickson, E. J. Kramer, C. J. Hawker, Evolution of Block Copolymer Lithography to Highly Ordered Square Arrays, *Science* **2008**, *322*, 429.
- 9 T. Kato, M. Yoshio, T. Ichikawa, B. Soberats, H. Ohno, M. Funahashi, Transport of ions and electrons in nanostructured liquid crystals, *Nat. Rev. Mater.* **2017**, *2*, 17001.
- 10 S. Sergeyev, W. Pisula, Y. H. Geerts, Discotic liquid crystals: a new generation of organic semiconductors. *Chem. Soc. Rev.* **2007**, *36*, 1902.
- 11 M. O'Neill, S. M. Kelly, Ordered Materials for Organic Electronics and Photonics, *Adv. Mater.* **2011**, *23*, 566–584.

-
- 1 12 W. Pisula, M. Zorn, J. Y. Chang, K. Müllen, R. Zentel, Liquid Crystalline Ordering and
2 Charge Transport in Semiconducting Materials; *Macromol. Rapid Commun.* **2009**, *30*,
3 1179–1202.
4
5
6 13 M. Kumar, S. Kumar, Liquid crystals in photovoltaics: a new generation of organic
7 photovoltaics, *Polymer Journal* **2017**, *49*, 85–111.
8
9
10 14 Q. Li, *Nanoscience with liquid crystals*, Springer, Cham, **2014**.
11
12 15 C. Tschierske, G. Ungar, Mirror Symmetry Breaking by Chirality Synchronization in
13 Liquids and Liquid Crystals of Achiral Molecules, *Chem PhysChem.* **2016**, *17*, 9-26.
14
15 16 H. J. Lu, X. B. Zeng, G. Ungar, C. Dressel, C. Tschierske, Solution of the Puzzle of
17 Smectic-Q: The Phase Structure and the Origin of Spontaneous Chirality, *Angew. Chem.*
18 *Int. Ed.* **2018**, *57*, 2835-2840.
19
20
21 17 C. Tschierske, Development of Structural Complexity by Liquid-Crystal Self-assembly.
22 *Angew. Chem., Int. Ed.* **2013**, *52*, 8828–8878.
23
24
25 18 H.-S. Kitzerow, C. Bahr, *Chirality in Liquid Crystals*, Springer, New York, **2001**.
26
27 19 I. Nishiyama, Remarkable Effect of Pre-organization on the Self Assembly in Chiral
28 Liquid Crystals, *Chem Rec.* **2009**, *9*, 340–355.
29
30 20 J.-F. Sadoc, R. Mosseri, *Geometrical frustration*, Cambridge University Press,
31 Cambridge, *1999*.
32
33
34 21 M.-H. Yen, J. Chairapa, X. B. Zeng, Y. Liu, L. Cseh, G. H. Mehl, G. Ungar, Added
35 Alkane Allows Thermal Thinning of Supramolecular Columns by Forming Superlattice
36 - An X-ray and Neutron Study. *J. Am. Chem. Soc.* **2016**, *138*, 5757–5760.
37
38
39 22 F. Tournilhac, L. M. Blinov, J. Simon, S. V. Yablonsky *Nature*, **1992**, *359*, 621-623.
40
41 23 G. Ungar, C. Tschierske, V. Abetz, R. Holyst, M. A. Bates, F. Liu, M. Prehm, R.
42 Kieffer, X. Zeng, M. Walker, B. Glettner, A. Zywockinski, Self-Assembly at Different
43 Length Scales: Polyphilic Star-Branched Liquid Crystals and Miktoarm Star
44 Copolymers. *Adv. Funct. Mater.* **2011**, *21*, 1296–1323.
45
46
47 24 S. Poppe, M. Poppe, H. Ebert, M. Prehm, C. Chen, F. Liu, S. Werner, K. Bacia, C.
48 Tschierske, Effects of Lateral and Terminal Chains of X-shaped Bolapolyphiles with
49 Oligo(phenylene ethynylene) Cores on Self-assembly Behaviour Part 1: Transition
50 between Amphiphilic and Polyphilic Self-assembly in the Bulk, *Polymers* **2017**, *9*, 471.
51
52
53
54
55 25 X. Mang, X. Zeng, B. Tang, F. Liu, G. Ungar, R. Zhang, L. Cseh, and G. H. Mehl,
56 Control of anisotropic self-assembly of gold nanoparticles coated with mesogens, *J.*
57 *Mater. Chem.* **2012**, *22*, 11101-11106.
58
59
60
61
62
63
64
65

-
- 1 26 W. Lewandowski, M. Wojcik, and E. Gorecka, Metal nanoparticles with liquid-
2 crystalline ligands: Controlling nanoparticle superlattice structure and properties,
3 *ChemPhysChem*. **2014**, *15*, 1283-1295.
4
5
6 27 J. P.F. Lagerwall, G. Scalia, *Liquid Crystals with Nano and Microparticles*, World
7 Scientific, New Yersey, **2017**.
8
9
10 28 X. H. Cheng, M. Prehm, M. K. Das, J. Kain, U. Baumeister, S. Diele, D. Leine, A.
11 Blume, C. Tschierske, Calamitic Bolaamphiphiles with (Semi)Perfluorinated Lateral
12 Chains: Polyphilic Block Molecules with New Liquid Crystalline Phase Structures. *J.*
13 *Am. Chem. Soc.* **2003**, *125*, 10977-10996.
14
15
16 29 C. Tschierske, Liquid crystal engineering - new complex mesophase structures and their
17 relations to polymer morphologies, nanoscale patterning and crystal engineering. *Chem.*
18 *Soc. Rev.* **2007**, *36*, 1930–1970.
19
20
21 30 C. Tschierske, C. Nürnberger, H. Ebert, B. Glettner, M. Prehm, F. Liu, X. B. Zeng, G.
22 Ungar, Complex tiling patterns in liquid crystals. *Interface Focus* **2012**, *2*, 669–680.
23
24
25 31 M. Prehm, C. Enders, M. Yahyaee-Anzahae, B. Glettner, U. Baumeister, C.
26 Tschierske, Distinct Columnar and Lamellar Liquid Crystalline Phases Formed by New
27 Bolaamphiphiles with Linear and Branched Lateral Hydrocarbon Chains. *Chem. Eur. J.*
28 **2008**, *14*, 6352–6368.
29
30
31 32 M. Prehm, F. Liu, U. Baumeister, X. Zeng, G. Ungar, C. Tschierske, The Giant-
32 Hexagon Cylinder Network - A Liquid-Crystalline Organization Formed by a T-Shaped
33 Quaternary Amphiphile. *Angew. Chem. Int. Ed.* **2007**, *46*, 7972–7975
34
35
36 33 M. Prehm, X.-H. Cheng, S. Diele, M.-K. Das, C. Tschierske, New Liquid Crystalline
37 Phases with Layerlike Organization. *J. Am.- Chem. Soc.* **2002**, *124*, 12072-12073.
38
39
40 34 X. H. Cheng, M. K. Das, S. Diele, C. Tschierske, Novel Liquid-Crystalline Phases with
41 Layerlike Organization. *Angew. Chem. Int. Ed.* **2002**, *41*, 4031-4035.
42
43
44 35 X. Cheng, M. K. Das, U. Baumeister, S. Diele, C. Tschierske, Liquid Crystalline
45 Bolaamphiphiles with Semiperfluorinated Lateral Chains: Competition between
46 Layerlike and Honeycomb-Like Organization, *J. Am. Chem. Soc.* **2004**, *126*, 12930-
47 12940.
48
49
50 36 R. Kieffer, M. Prehm, K. Pelz, U. Baumeister, F. Liu, H. Hahn, H. Lang, G. Ungar, C.
51 Tschierske, Siloxanes and carbosilanes as new building blocks for T-shaped
52 bolaamphiphilic LC molecules. *Soft Matter*, **2009**, *5*, 1214–1227.
53
54
55
56
57
58
59
60
61
62
63
64
65

-
- 1 37 F. Liu, M. Prehm, X. Zeng, C. Tschierske, G. Ungar, Skeletal Cubic, Lamellar, and
2 Ribbon Phases of Bundled Thermotropic Bolapolyphiles. *J. Am. Chem. Soc.* **2014**, *136*,
3 6846–6849.
4
5
6 38 X. Zeng, M. Prehm, G. Ungar, C. Tschierske, F. Liu, Formation of a Double Diamond
7 Cubic Phase by Thermotropic Liquid Crystalline Self-Assembly of Bundled
8 Bolaamphiphiles. *Angew. Chem. Int. Ed.* **2016**, *55*, 8324-8327.
9
10 39 M. Prehm, F. Liu, X. Zeng, G. Ungar, C. Tschierske, Axial-bundle phases – new modes
11 of 2D, 3D, and helical columnar self-assembly in liquid crystalline phases of
12 bolaamphiphiles with swallow tail lateral chains. *J. Am. Chem. Soc.* **2011**, *133*, 4906-
13 4916.
14
15 40 F. Liu, M. Prehm, X. Zeng, G. Ungar, C. Tschierske, Two- and Three-Dimensional
16 Liquid-Crystal Phases from Axial Bundles of Rodlike Polyphiles: Segmented Cylinders,
17 Crossed Columns, and Ribbons between Sheets. *Angew. Chem. Int. Ed.* **2011**, *50*, 10599
18 –10602.
19
20 41 A. J. Crane, F. J. Martinez-Veracoechea, F. A. Escobedo, E. A. Muller, Molecular
21 Dynamics Simulation of the Mesophase Behaviour of A Model Bolaamphiphilic Liquid
22 Crystal with A Lateral Flexible Chain. *Soft Matter* **2008**, *4*, 1820–1829.
23
24 42 M. A. Bates, M. Walker, Dissipative Particle Dynamics Simulation of T- and X-Shaped
25 Polyphilic Molecules Exhibiting Honeycomb Columnar Phases. *Soft Matter* **2009**, *5*,
26 346–353.
27
28 43 T. D. Nguyen, S. C. Glotzer, Reconfigurable Assemblies of Shape-Changing Nanorods.
29 *ACS Nano* **2010**, *4*, 2585–2594.
30
31 44 X. Liu, K. Yang, H. Guo, Dissipative Particle Dynamics Simulation of the Phase
32 Behavior of T-Shaped Ternary Amphiphiles Possessing Rodlike Mesogens. *J. Phys.*
33 *Chem. B* **2013**, *117*, 9106–9120.
34
35 45 Y. Sun, P. Padmanabhan, M. Misra, F. A. Escobedo, Molecular dynamics simulation of
36 thermotropic bolaamphiphiles with a swallow-tail lateral chain: formation of cubic
37 network phases. *Soft Matter* **2017**, *13*, 8542-8555.
38
39 46 S. George, C. Bentham, X. B. Zeng, G. Ungar, G. A. Gehring, “Monte Carlo study of
40 the ordering in a strongly frustrated liquid crystal”, *Phys. Rev. E*, **2017**, *95*, 062126.
41
42 47 S.-M. Park, G. S. W. Craig, Y.-H. La, H. H. Solak, P. F. Nealey, Square Arrays of
43 Vertical Cylinders of PS-*b*-PMMA on Chemically Nanopatterned Surfaces.
44 *Macromolecules* **2007**, *40*, 5084-5094
45
46
47
48
49
50
51
52
53
54
55
56
57
58
59
60
61
62
63
64
65

-
- 1 48 H. K. Choi, J. Gwyther, I. Manners, C. A. Ross, Square Arrays of Holes and Dots
2 Patterned from a Linear ABC Triblock Terpolymer *ACS Nano* **2012**, *6*, 8342–8348; K.
3 Aissou, H. K. Choi, A. Nunns, I. Manners, C. A. Ross, Ordered Nanoscale
4 Archimedean Tilings of a Templated 3–Miktoarm Star Terpolymer. *Nano Lett.* **2013**,
5 *13*, 835–839.
6
7
8
9
10 49 K. Yue, C. Liu, M. Huang, J. Huang, Z Zhou, K. Wu, H Liu, Z. Lin, A.-C. Shi, W.-B.
11 Zhang, S. Z. D. Cheng, Self-Assembled Structures of Giant Surfactants Exhibit a
12 Remarkable Sensitivity on Chemical Compositions and Topologies for Tailoring Sub-
13 10 nm Nanostructures, *Macromolecules* **2017**, *50*, 303–314.
14
15
16
17 50 J. Kwak, A. K. Mishra, J. Lee, K. S. Lee, C. Choi, S. Maiti, M. Kim, J. K. Kim,
18 Nanolithography Fabrication of Sub-3 nm Feature Size Based on Block Copolymer
19 Self- Assembly for Next-Generation, *Macromolecules* **2017**, *50*, 6813–6818.
20
21
22
23 51 H. Mukai, M. Yokokawa, M. Ichihara, K. Hatsusaka, K. Ohta, Discotic liquid crystals
24 of transition metal complexes 42^{\dagger} : the detailed phase structures and phase transition
25 mechanisms of two Cub mesophases shown by discotic liquid crystals based on
26 phthalocyanine metal complexes, *J. Porphyrins Phthalocyanines* **2010**, *14*, 188–197.
27
28
29
30 52 Y. Chinoa, K. Ohta, M. Kimurab, M. Yasutake, Discotic liquid crystals of transition
31 metal complexes, 53^{\dagger} : synthesis and mesomorphism of phthalocyanines substituted by
32 *m*-alkoxyphenylthio groups, *J. Porphyrins Phthalocyanines* **2017**, *21*, 159–178.
33
34
35
36 53 R. Kieffer, M. Prehm, B. Glettner, K. Pelz, U. Baumeister, F. Liu, X. Zeng, G. Ungar,
37 C. Tschierske, X-Shaped polyphilics: liquid crystal honeycombs with single-molecule
38 walls. *Chem. Commun.* **2008**, 3861–3863.
39
40
41
42 54 M. Poppe, C. Chen, F. Liu, M. Prehm, S. Poppe, C. Tschierske, Emergence of tilt in
43 square honeycomb liquid crystals. *Soft Matter* **2017**, *13*, 4676–4680.
44
45
46
47 55 B. Chen, U. Baumeister, S. Diele, M. K. Das, X. Zeng, G. Ungar, C. Tschierske, A New
48 Type of Square Columnar Liquid Crystalline Phases Formed by Facial Amphiphilic
49 Triblock Molecules. *J. Am. Chem. Soc.* **2004**, *126*, 8608–8609.
50
51
52
53 56 X. Cheng, F. Liu, X. Zeng, G. Ungar, J. Kain, S. Diele, M. Prehm, C. Tschierske,
54 Influence of Flexible Spacers on Liquid-Crystalline Self-Assembly of T-Shaped
55 Bolaamphiphiles, *J. Am. Chem. Soc.* **2011**, *133*, 7872–7881.
56
57
58
59 57 S. Poppe, A. Lehmann, A. Scholte, M. Prehm, X. Zeng, G. Ungar, C. Tschierske,
60 Zeolite-like liquid crystals. *Nat. Commun.* **2015**, *6*, 8637.
61
62
63
64
65

-
- 1 58 X. Zeng, R. Kieffer, B. Glettner, C. Nürnberger, F. Liu, K. Pelz, M. Prehm, U.
2 Baumeister, H. Hahn, H. Lang, G. A. Gehring, C. H. M. Weber, J. K. Hobbs, C.
3 Tschierske, G. Ungar, Complex Multicolor Tilings and Critical Phenomena in
4 Tetraphilic Liquid Crystals. *Science* **2011**, *331*, 1302–1306.
5
6
7
8 59 F. Liu, R. Kieffer, X. Zeng, K. Pelz, M. Prehm, G. Ungar, C. Tschierske, Arrays of
9 giant octagonal and square cylinders by liquid crystalline self-assembly of X-shaped
10 polyphilic molecules. *Nat. Commun.* **2012**, *3*, 1104.
11
12
13 60 J. P. Wagner, P. R. Schreiner, London Dispersion in Molecular Chemistry-
14 Reconsidering Steric Effects. *Angew. Chem. Int. Ed.* **2015**, *54*, 12274 – 12296.
15
16
17 61 A. Zielinska, M. Leonowicz, H. Li, T. Nakanishi, Controlled self-assembly of alkylated-
18 π compounds for soft materials — Towards optical and optoelectronic applications
19 *Current Opinion in Colloid & Interface Science* **2014**, *19*, 131–139.
20
21
22 62 N. Miyaura, T. Yanagi, A. Suzuki, The Palladium-Catalyzed Cross-Coupling Reaction
23 of Phenylboronic Acid with Haloarenes in the Presence of Bases. *Synth. Commun.* **1981**,
24 *11*, 513-519.
25
26
27 63 M. Kölbel, T. Beyersdorff, C. Tschierske, S. Diele, J. Kain, Thermotropic and Lyotropic
28 Liquid Crystalline Phases of Rigid Aromatic Amphiphiles. *Chem. Eur. J.* **2000**, *6*, 3821-
29 3837.
30
31
32 64 M. Kölbel, T. Beyersdorff, X. Cheng, C. Tschierske, J. Kain, S. Diele, Design of Liquid
33 Crystalline Block Molecules with Nonconventional Mesophase Morphologies:
34 Calamitic Bolamphiphiles with Lateral Alkyl Chains. *J. Am. Chem. Soc.* **2001**, *123*,
35 6809-6818.
36
37
38 65 R. V. Henley, E. E. Turner, The scission of diaryl ethers and related compounds by
39 means of piperidine. Part III. The nitration of 2:4-dibromo-2':4'-dinitrophenyl ether and
40 of 2:4-dibromophenyl *p*-toluenesulphonate and benzoate. The chlorination and
41 bromination of *m*-nitrophenol. *J. Chem. Soc.*, 1930, 928-940.
42
43
44 66 H. Liu, M. Bernhardsen, A. Fiksdahl, Polybrominated diphenyl ethers (BDEs);
45 preparation of reference standards and fluorinated internal analytical standards.
46 *Tetrahedron* **2006**, *62*, 3564-3572.
47
48
49 67 B. Chen, X. B. Zeng, U. Baumeister, S. Diele, G. Ungar, C. Tschierske, Liquid Crystals
50 with Complex Superstructures, *Angew. Chem. Int. Ed.* **2004**, *43*, 4621-4625.
51
52
53 68 B. Chen, X. Zeng, U. Baumeister, G. Ungar, C. Tschierske, Liquid Crystalline
54 Networks Composed of Pentagonal, Square, and Triangular Cylinders. *Science* **2005**,
55 *307*, 96–99.
56
57
58
59
60
61
62
63
64
65

-
- 1 69 X. Cheng, X. Dong, G. Wei, M. Prehm, C. Tschierske, Liquid-Crystalline Triangle
2 Honeycomb Formed by a Dithiophene-Based X-Shaped Bolaamphiphile. *Angew. Chem.*
3 *Int. Ed.* **2009**, *48*, 8014–8017.
4
5
6 70 X. Cheng, H. Gao, X. Tan, X. Yang, M. Prehm, H. Ebert, C. Tschierske, Transition
7 between triangular and square tiling patterns in liquid-crystalline honeycombs formed
8 by tetrathiophene-based bolaamphiphiles. *Chem. Sci.* **2013**, *4*, 3317–3331.
9
10
11 71 F. Liu, B. Chen, B. Glettner, Marko Prehm, Malay Kumar Das, Ute Baumeister,
12 Xiangbing Zeng, Goran Ungar, C. Tschierske, The Trapezoidal Cylinder Phase: A New
13 Mode of Self-Assembly in Liquid-Crystalline Soft Matter. *J. Am. Chem. Soc.* **2008**, *130*,
14 9666–9667.
15
16
17
18
19
20
21
22
23
24
25
26
27
28
29
30
31
32
33
34
35
36
37
38
39
40
41
42
43
44
45
46
47
48
49
50
51
52
53
54
55
56
57
58
59
60
61
62
63
64
65